HHS Public Access

Author manuscript

Cell Rep Phys Sci. Author manuscript; available in PMC 2023 February 16.

Published in final edited form as:

Cell Rep Phys Sci. 2022 October 19; 3(10): . doi:10.1016/j.xcrp.2022.101067.

Polynorbornene-based bioconjugates by aqueous grafting-from ring-opening metathesis polymerization reduce protein immunogenicity

Derek C. Church[1,7], **Elizabathe Davis**[1,7], **Adam A. Caparco**[1], **Lauren Takiguchi**[1], **Young Hun Chung**[4], **Nicole F. Steinmetz**[1,2,3,4,5,6], **Jonathan K. Pokorski**[1,2,3,8,*]

[1]Department of NanoEngineering, University of California, San Diego, La Jolla, CA 92093, USA

[2]Center for Nano-ImmunoEngineering, University of California, San Diego, La Jolla, CA 92093, USA

[3]Institute for Materials Discovery and Design, University of California, San Diego, La Jolla, CA 92093, USA

[4]Department of Bioengineering, University of California, San Diego, La Jolla, CA 92093, USA

[5]Department of Radiology, University of California, San Diego, La Jolla, CA 92093, USA

[6]Moores Cancer Center, University of California, San Diego, La Jolla, CA 92093, USA

[7]These authors contributed equally

[8]Lead contact

SUMMARY

Protein-polymer conjugates (PPCs) improve therapeutic efficacy of proteins and have been widely used for the treatment of various diseases such as cancer, diabetes, and hepatitis. PEGylation is considered as the “gold standard” in bioconjugation, although in practice its clinical applications are becoming limited because of extensive evidence of immunogenicity induced by pre-existing anti-PEG antibodies in patients. Here, optimized reaction conditions for living aqueous grafting-from ring-opening metathesis polymerization (ROMP) are utilized to synthesize water-soluble polynorbornene (PNB)-based PPCs of lysozyme (Lyz-PPCs) and bacteriophage Qβ (Qβ-PPCs) as PEG alternatives. Lyz-PPCs retain nearly 100% bioactivity and Qβ-PPCs exhibit up to 35% decrease in protein immunogenicity. Qβ-PPCs derived from NB-PEG show no reduction in

*Correspondence: jpokorski@ucsd.edu.

AUTHOR CONTRIBUTIONS

D.C.C. and E.D. synthesized and characterized Lyz-PPCs and Qβ-PPCs, respectively. D.C.C and E.D. synthesized and characterized NB-PEG and NB-Zwit monomers. D.C.C. and E.D. contributed to manuscript writing. A.A.C. performed characterizations such as DLS, TEM, and ELISA immunoassay. Y.H.C. performed the expression of Qβ bacteriophage. L.T. was involved in the synthesis of Lyz-PPCs. J.K.P. and N.F.S. provided expertise and feedback during the project and editing, and review of the article. J.K.P. and N.F.S. acquired funding.

SUPPLEMENTAL INFORMATION

Supplemental information can be found online at https://doi.org/10.1016/j.xcrp.2022.101067

DECLARATION OF INTERESTS

The authors declare no competing interests.

recognition by anti-PEG antibodies while Qβ-PPCs derived from NB-Zwit show >95% reduction as compared with Qβ-PEG. This work demonstrates a new method for PPC synthesis and the utility of grafting from PPCs to evade immune recognition.

Graphical Abstract

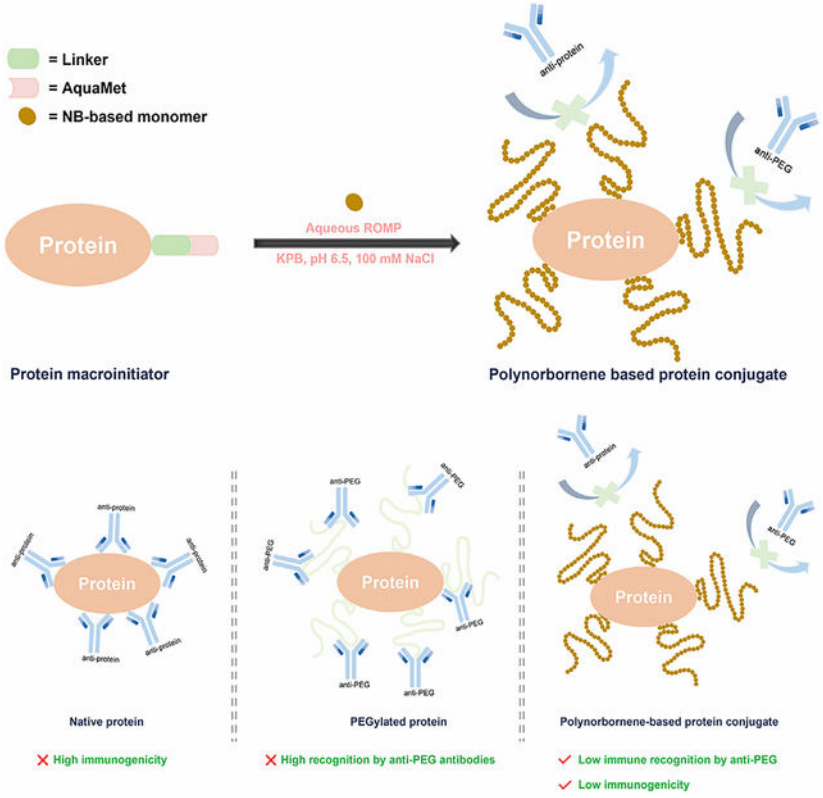

Church and Davis et al. report the synthesis of water-soluble protein-polymer conjugates (PPCs) by aqueous grafting-from ring-opening metathesis polymerization for protein therapeutics. PPCs evade recognition by protein-specific and PEG-specific antibodies and could be a potential PEG alternative in protein therapeutics.

INTRODUCTION

Protein therapeutics has been a vital tool in the treatment of various diseases such as cancer, diabetes, and hepatitis.[1–4] However, these biologics in their native form can suffer from immunogenicity, poor blood circulation half-life, and low protein stability due to degradation, leading to premature clearance, low bioavailability, and loss of efficacy. Therefore, protein-polymer conjugates (PPCs) play an important role in addressing these challenges.[5–7] By attaching polymers to the protein surface, the overall molecular weight of the conjugate is increased, limiting renal clearance and thereby increasing the blood circulation half-life.[8,9] Furthermore, covalently attached polymers can sterically shield the biologic from binding by opsonin proteins, antibodies, and proteolytic enzymes, which the host immune system can utilize to eliminate foreign material.[9–11]

PPCs for therapeutic applications have predominantly been synthesized by the covalent attachment of polyethylene glycol (PEG) to the protein surface (PEGylation).[12–14] Modifying therapeutic proteins with PEG has been effective at increasing drug efficacy, resulting in more than 24 Food and Drug Administration (FDA)-approved drugs since 1990.[15] However, it has been observed that some of these therapeutic PEG conjugates, notably PEG-uricase (Krystexxa, treatment of chronic gout)[16,17] and PEG-asparaginase (Oncaspar, treatment of acute lymphoblastic leukemia)[18] undergo "accelerated blood clearance." This has been attributed to anti-PEG antibodies, which pre-exist in approximately 70% of the general population.[19–22] Studies have shown that these antibodies bind to structural motifs on the PEG portion of the PPC, resulting in loss of protein activity, reduced safety, and accelerated clearance of the therapeutics.[18,21,23–25] Moreover, there are two reports of anaphylaxis reaction to Pfizer/BioNTech COVID-19 vaccine in individuals with PEG hypersensitivity.[26,27] The utility of PEG is also limited from a materials design perspective because it does not contribute to further functionalization of protein biologics such as the simultaneous incorporation of targeting peptides or small-molecule therapeutics.[28] Furthermore, PEG is limited to end-group functionalization, limiting the chemical diversity that PPCs can achieve. Therefore, studying PPCs derived from alternative biocompatible polymers is essential for the progress of protein therapeutics.

There are traditionally two methods for the synthesis of PPCs: grafting-to and grafting-from.[29–34] In the grafting-to method, which is used in the synthesis of PEGylated protein biologics, a polymer chain with a reactive end group is conjugated to the protein surface at amino acids with complementary reactivity. Thus, polymers can be synthesized, modified, and characterized using well-developed organic and polymer chemistry methods. Using similar bioconjugation strategies, the grafting-from approach first conjugates an initiator directly onto the protein surface, forming a protein macroinitiator. Under initiating conditions and in the presence of monomer, the polymer chain grows outwardly from the protein surface. Compared with the grafting-to approach in which high-molecular-weight polymers are used to functionalize the protein, greater polymer densities on the protein surface can be achieved with the grafting-from methodology owing to favorable kinetic and thermodynamic reaction parameters.[35,36] Additionally, purification is simpler because of the large disparity in size between monomer and conjugate.

Grafting-from polymerizations generally rely on controlled radical polymerization techniques such as reversible addition-fragmentation transfer (RAFT)[37–39] and atom transfer radical polymerization (ATRP)[40] to control the dispersity of the polymer chains and the overall molecular weight of the PPC. However, RAFT and ATRP can be difficult to carry out because exogenous oxygen terminates radical polymerization processes. While these effects can be mitigated, multicomponent reaction conditions and relatively complex experimental setups are required and limit their widespread use beyond polymer chemistry fields.[40,41] Our lab has used the exceptional capabilities of ring-opening metathesis polymerization (ROMP) to integrate highly functional polymers at biological interfaces.[10,42–44] ROMP in organic solvents can be conducted under ambient conditions without the need to exclude oxygen, and is functional group tolerant and amenable to block copolymer formation thanks to high ruthenium end-group fidelity. However, ROMP under aqueous conditions, particularly those compatible with the synthesis of PPCs, has been underdeveloped. Traditional aqueous

ROMP conditions require organic cosolvents or extremely low pH to achieve high monomer conversion.[45–52] Unfortunately, these conditions are not compatible with protein stability.

In our current study we describe the synthesis of PPCs derived from lysozyme and bacteriophage Qβ by using a grafting-from aqueous ROMP approach. Initial efforts from our lab to synthesize PPCs in this manner using neutral pH conditions were met with modest success as poor initiation efficiency was observed in all but the highest monomer loadings.[42] Recently, Church et al. demonstrated that ROMP can be conducted at neutral pH under ambient conditions and without the addition of organic cosolvents by the addition of simple chloride salts.[53] Chloride concentration has a profound effect on aqueous polymerizations, increasing catalyst stability and yielding high monomer conversions and molecular weight control.[53,54] Using this improved biocompatible method, we describe the application of this methodology to improve the polymerization and scope of aqueous grafting-from ROMP for the synthesis of PPCs and demonstrate their ability to retain high protein activity and suppress immune recognition of a carrier protein using polynorbornene (PNB) polymers.

RESULTS AND DISCUSSION

Synthesis of grafting-from lysozyme protein-polymer conjugates

We have previously demonstrated that a pH between 6.5 and 7.4 as well as a NaCl concentration of 100 mM were optimal conditions for aqueous ROMP, which resulted in rapid polymerization and high conversion of water-soluble norbornene (**NB**) monomers.[53] We next sought to utilize similar conditions to optimize the synthesis of PPCs made via a ROMP grafting-from approach. *cis*-5-Norbornene-*exo*-2,3-dicarboxylic anhydride (exo-NBDA) was first conjugated to free lysines on the surface of **Lyz** to generate **Lyz-NB** yielding ~4–5 modifications per protein (Figures S1 and S2).[42] The importance of pH and chloride concentration on the grafting-from polymerization was then assessed in buffered solution at pH 6.5 or 7.4 and in the presence or absence of NaCl. Macroinitiator (MI) formation and polymerization using an NB PEG imide monomer (NB-PEG) under these conditions were conducted according to Figure 1A. NB-PEG was reacted with 0, 20, 30, 50, and 100 equiv relative to NBs on the modified protein surface. Synthesis of lysozyme protein-polymer conjugate Lyz-PPC was verified by SDS-PAGE and size-exclusion chromatography (SEC).

Interestingly, at pH 7.4 with 100 mM NaCl, no conjugates were observed for any monomer loading level (Figure 1B), despite our previous work demonstrating that aqueous ROMP polymerizations with high monomer conversion can be achieved under these conditions.[53] Synthesis of the free polymer in the presence of lysozyme under these conditions proceeded smoothly with 99% monomer conversion (Figure S3). This discrepancy may be due to the reactivity of pH-sensitive amino acid side chains present near the ruthenium catalyst center on the macroinitiator, potentially deactivating the catalytic center. Fortunately, lowering the buffer pH to6.5 produced Lyz-PPC1 with excellent initiation efficiency and control over the molecular weight as a function of monomer loading. This is observed by a gradual shift to higher molecular weights in the SDS-PAGE gels as well as a shift to lower retention volumes in the SEC as the monomer loading is increased (Figures 1B, 1C, and S4). Furthermore, these ROMP grafting-from polymerizations are rapid, reaching full conversion

within 20 min (Figure 1D). When the chloride source is excluded from the buffered solution (pH 6.5) no polymerization is observed, consistent with our previous observations (Figure S5). We have previously demonstrated that excluding chloride from the reaction medium causes the rapid generation of catalytically inactive ruthenium hydroxide complexes. The addition of excess chloride shifts the equilibrium away from the inactive species and toward the metathesis active dichloro complex.

Monomer scope for grafting-from ROMP PPCs

With these optimized conditions in hand, expansion of the monomer scope was explored by targeting the synthesis of Lyz-PPC2 and Lyz-PPC3 utilizing a zwitterionic norbornene (NB-Zwit) and an oxanorbornene PEG imide (oNB-PEG) monomer, respectively. Synthesis of Lyz-PPC2 exhibited good molecular weight control as determined by SDS-PAGE and SEC (Figures 2A and S6). In contrast, poor conversions were observed for the synthesis of **Lyz-PPC3** (Figure 2B). This is consistent with our previous work demonstrating significantly lower monomer conversion of oxanorbornene monomers relative to analogous NB monomers.[53] Additionally, after the successful synthesis of Lyz-PPC1 and Lyz-PPC2 we observed a 90.8% and 84.6% retention of protein activity, respectively compared with Lyz (Figure S7).

Incorporating functional monomers into the polymer chain that impart new activities to therapeutic proteins could be an important advancement for next-generation PPCs. One route to achieve this is by utilizing a block copolymer architecture to position these targeting moieties at the polymer chain end of the PPC. Catalyst fidelity and living characteristics of the polymerization were evaluated with this potential goal in mind. NB-Zwit was added to lysozyme macroinitiator Lyz-MI with aliquots removed after 20 and 25 min of reaction (Figure 3A). No change in the molecular weight was observed by SEC, which could signify either complete monomer consumption or a deactivated catalyst (Figure 3B). NB-PEG was then added and allowed to react for a further 20 min. A shift to lower retention volumes indicated a large change in molecular weight and successful block copolymer formation (Figure 3B). These results demonstrate that under these conditions the ruthenium catalyst remains active on the chain end throughout the course of the reaction, allowing for the synthesis of block polymer architectures in PPCs.

To demonstrate that bioactive small molecules can be incorporated into a block copolymer architecture and remain functional, a biotin functionalized norbornene monomer (NB-biotin) was incorporated as the terminal block in Lyz-PPC-biotin and its ability to bind to a fluorescently labeled streptavidin (Stv488) was compared with that of Lyz-PPC1 (Reaction scheme S2 and Figure 4). Fluorescent PAGE analysis shows that in the absence of a biotinylated polymer, no binding is observed and only the Stv488 band is observed (far-right lane). However, when Stv488 is included with a biotinylated polymer (Lyz-PPC-biotin), the strong Stv488 band disappears and the fluorescence signal is distributed across the band associated with the PPC, indicating binding to Stv488 (second lane from right). This demonstrated the feasibility of our ROMP grafting-from methodology to incorporate bioactive small molecules into PPCs.

Synthesis of grafting-from Qβ PPCs: Nanocarrier conjugates

Our previous work demonstrated that water-soluble poly(NB-PEG) polymers conjugated to protein nanoparticles by a grafting-to approach improved protection from anti-protein antibodies when compared with linear PEG.[10] We therefore wanted to compare the immune shielding capabilities of PPCs made by an aqueous ROMP grafting-from methodology. Qβ bacteriophage has been explored for applications such as drug delivery, vaccine platforms, immunotherapy, and imaging.[55,56] Qβ is a 28 nm icosahedral virus-like particle (VLP) made up of 180 copies of monomeric coat proteins and served as a test bed in our previous studies, making it a useful comparator for the grafting-from methodology. Each Qβ coat protein has four free primary amines per coat protein (720 per VLP) available for modification, which were first modified by exo-NBDA to obtain Qβ-NB (Figure S11). Mass spectroscopy analysis indicated an average of ~1–2 modifications per coat protein when 30 equiv of exo-NBDA per amine residue were used (Figure S10). This was followed by the synthesis of grafting-from Qβ-PPC1 and Qβ-PPC2 from the monomers NB-PEG and NB-Zwit, respectively (Figure 5A). Monomer equivalents of 30 and 100 per Qβ coat protein yielded four different grafting-from Qβ-PPCs: Qβ-PPC1–30, Qβ-PPC1–100, Qβ-PPC2–30, and Qβ-PPC2–100.

The successful syntheses of grafting-from Qβ-PPCs were confirmed by denaturing SDS-PAGE. The denaturing SDS-PAGE (Figure 5B) indicated efficient grafting of the polymers to Qβ. Colocalization of the bands was observed for Qβ-PPCs and a decrease in the mobility of the conjugate bands was observed with higher monomer loading, which indicated a higher molecular weight. Small amounts of unreacted Qβ/Qβ-NB coat proteins were also observed after conjugations and could be potentially due to the presence of unmodified Qβ coat proteins or uninitiated species (Figure S10B). The SDS-PAGE was additionally treated with iodine to stain Qβ-PPC1 (Figure S12), which is the result of formation of iodide complexes with PEG,[57] and the colocalization of bands further confirmed the grafting-from polymerization. SEC of Qβ-PPCs (Figure 5C) indicated higher retention volumes compared with Qβ and Qβ-NB. These data are contrary to the expected trend, although consistent with our previous observation in the grafting-to PNB-based Qβ conjugates synthesized in our lab.[43] This is likely due to the interaction of PNB-based polymers with the material in the column, potentially driven by the unique “raspberry” conformation associated with Qβ-PNB conjugates.[10] It is also important to point out that the unreacted Qβ/Qβ-NB coat proteins observed in SDS-PAGE are not detected in SEC, as the Qβ-PPCs elute as a whole particle while Qβ-PPCs are denatured for SDS-PAGE. Dynamic light scattering (DLS) and transmission electron microscopy (TEM) were carried out to confirm Qβ structural integrity after grafting-from conjugation. DLS measurements of all the conjugates (Figure S14) showed increases in size compared with native Qβ. The hydrodynamic size of the Qβ-PPC1 increased from68.1 nm to 142 nm as we increased monomer loadings of NB-PEG from 30 to 100 equiv. Similarly, when the NB-Zwit monomer loadings were increased from 30 to 100 equiv, an increase in the hydrodynamic size from 59.2 nm to 91.3 nm was observed. The broad peaks seen in the DLS measurements are not uncommon for a polydisperse population of self-associating polymers.[58] TEM micrographs of the conjugates (Figures 5D–5G) further verified Qβ structural integrity after the grafting-from ROMP polymerization. The presence of polymer affects the quality of the negative stain by uranyl acetate, altering

the contrast with the background, which has been previously reported in TEM samples using polymers.[59]

Immune recognition of Qβ-PPCs by anti-Qβ and anti-PEG antibodies

After the successful synthesis of Qβ-PPCs, the immune shielding capabilities of the grafting-from PPCs were evaluated by ELISAs, detecting response against either Qβ or PEG. As a control, we covalently conjugated PEG-10 kDa using a traditional grafting-to conjugation scheme to prepare Qβ-PEG (Reaction scheme S4; Figures S13 and S14C). Since PEGylation is the standard method for preparing PPCs, this was used for comparison to demonstrate the effectiveness of immune shielding with grafting-from PPCs. The grafting-from ROMP polymerizations significantly reduced immune recognition by anti-Qβ antibodies compared with wild-type Qβ (Figure 6). Qβ-PPC1 and Qβ-PPC2 showed a 27.5%–30% and 30%–35% decrease in antibody recognition, respectively. Also, better protection from antibody recognition was observed in the case of Qβ-PPC1–100 and Qβ-PPC2–100 compared with Qβ-PPC1–30 and Qβ-PPC2–30, respectively. In contrast, the grafting-to Qβ-PEG conjugate showed no improvement in antibody shielding. It is also worth noting that Qβ-PPC2 showed better immunoshielding from anti-Qβ compared with Qβ-PPC1.[60,61] These are significant results because new alternatives for PEG will need to be rapidly advanced, as a greater proportion of the population has pre-existing anti-PEG antibodies rendering PEGylated drugs ineffective or resulting in side effects which could be quite severe.

There is extensive evidence of pre-existing anti-PEG antibodies in humans,[19–21] leading to adverse effects in patients treated with PEGylated therapeutics in clinical studies.[16–18,26,27] Therefore, recognition of Qβ-PPCs by anti-PEG antibodies was also investigated. As expected, the grafting-to Qβ-PEG produced the highest immune response and was used as the positive control. Qβ-PPC1 synthesized from NB-PEG monomers diminished the immune response of Qβ-PEG by 15%. This level of detection of Qβ-PPC1 by anti-PEG was unexpected, as PEG with up to 9 EG units have shown low PEG-specific antigenicity.[62] As hypothesized, Qβ-PPC2 derived from NB-Zwit monomer had negligible recognition by anti-PEG antibodies. Anti-PEG antibody recognition of Qβ-PPC2 showed <5% binding compared with Qβ-PEG. The effective reduction in recognition by anti-Qβ and its ability to evade recognition by anti-PEG makes Qβ-PPC2 particularly promising. Conjugation of zwitterionic polymers has been shown to retain high bioactivity of therapeutic proteins, which can be attributed to the superhydrophilicity of zwitterionic polymers.[61,63] While further investigation is required, we believe that protein bioconjugates derived from NB-Zwit hold great potential as an alternative to PEGylation in bioconjugation.

The current work developed a grafting-from aqueous ROMP protocol for the synthesis of water-soluble PPCs derived from NB-based monomers. We have demonstrated that pH 6.5 and elevated chloride concentrations increase the activity and lifetime of water-soluble ruthenium catalysts on the chain end of the PPC, providing control over Lyz-PPC and Qβ-PPC molecular weight as a function of monomer loading. These conditions can be utilized to incorporate a variety of diverse functional groups and water-soluble NB monomers into PPCs, including biologically active monomers containing biotin. The Qβ-PPCs maintained

particle integrity after the synthesis, as confirmed by TEM and DLS. Immune recognition studies of Qβ-PPCs demonstrated reduced protein immunogenicity and low PEG-specific antigenicity compared with grafting-to PEG conjugates. This suggests a better safety profile by grafting-from PNB-based bioconjugates compared with the extensively used grafting-to PEG conjugates. Particularly, the ability of the zwitterionic bioconjugate in evading immune recognition by both protein-specific and PEG-specific antibodies shows great promise. Additionally, with studies proving high retention of protein bioactivity and long systemic circulation of proteins conjugated with zwitterionic polymers, it holds great promise as a potential PEG alternative in protein-polymer conjugation.

EXPERIMENTAL PROCEDURES

Resource availability

Lead contact—Further information and requests for resources should be directed to and will be fulfilled by the lead contact, Jonathan K. Pokorski (jpokorski@ucsd.edu).

Materials availability—exo-NBDA,[64] NB-PEG,[53] NB-Zwit,[53] and oNB-PEG[44] were synthesized as previously described. All other reagents and solvents were used as obtained from commercial sources.

Data and code availability—The datasets generated in this study are available from the lead contact upon reasonable request.

Instrumentation

Molecular mass data were obtained using an Agilent 6230 Accurate-Mass time-of-flight mass spectrometry instrument with an in-line Agilent 1260 Infinity Binary liquid chromatograph. UV-visible (UV-vis) measurements were acquired using a Shimadzu BioSpecnano UV-vis spectrophotometer. DLS was conducted with a Malvern Panalytical Zetasizer Nano ZS at 25°C. Samples were diluted to 0.5 mg/mL in 10 mM potassium phosphate and transferred to an Eppendorf UVette disposable cuvette, and measurements were conducted with at least 12 runs per measurement for three measurements. SEC was performed using a GE Healthcare AKTA-FPLC 900 chromatography system equipped with a Superdex 75 10/300 GL size-exclusion column. For all SEC experiments, the mobile phase was PBS (pH 7.4) at a flow rate of 0.4 mL/min. SDS-PAGE was performed on GenScript ExpressPlus PAGE gels 4%–12% bis-tris protein gels (1.0 mm × 12 wells) (35 min, 140 V, 20× MES SDS running buffer). Samples were prepared with Novex LDS Sample Buffer (4×) and denatured at 95°C. Gels were stained with Coomassie SimplyBlue SafeStain (Life Technologies), and PEG-based conjugates were additionally stained by iodine solution. TEM of Qβ VLPs were performed on an FEI Tecnai G2 Spirit transmission electron microscope at 80 kV. Samples were diluted to 0.5 mg/mL in Milli-Q water for sample deposition. The solution was applied at a volume of 10 μL to FCF400-CU 400-mesh copper grids (Electron Microscopy Sciences, Hatfield, PA, USA) for 15 min at room temperature. The grids were washed three times for 30 s with Milli-Q water, and the sample was stained with 10 μL of 2% (w/v) uranyl acetate for 1 min. The grid was blotted to remove excess solution.

Synthesis of grafting-from Lyz-PPCs

Synthesis of Lyz-NB—Lysozyme (20 mg, 0.0014 mmol, 1.0 equiv) was dissolved in 7.2 mL of 0.1 M potassium phosphate buffer, pH 8.0. exo-NBDA (17.1 mg, 0.10 mmol, 75.0 equiv) in a solution of dimethyl sulfoxide (DMSO) (0.8 mL) was then added dropwise over 45 min using a syringe pump. The reaction mixture was stirred at room temperature for 18 h. The protein solution was then added to a 3500 molecular weight cutoff (MWCO) dialysis bag and stirred against 1 L of 10 mM potassium phosphate buffer (pH 6.5) with 100 mM NaCl. The buffer was exchanged twice over the course of 24 h. The protein solution was then concentrated using 6× 10,000 MWCO Amicon Ultra-4 mL Centrifugal Filter and centrifuged at 7,000 × *g* for 10 min. Final protein concentration was 2.6 mg/mL, determined using UV-vis spectroscopy and ε_{280} = 38,940 cm^{-1} M^{-1}. The resulting conjugates were analyzed by liquid chromatography/electron spray ionization/time-of-flight mass spectrometry and SEC. Lysozyme was modified with an average of 4–5 norbornenes (Figure S1). SEC displays a single monomodal peak (Figure S2).

General polymerization procedure for synthesis of Lyz-PPC1, Lyz-PPC2, and Lyz-PPC3—To a 1-mL solution of **Lyz-NB** at a concentration of 2 mg/mL in 10 mM potassium phosphate buffer (pH 6.5) in 100 mM NaCl (2.0 mg, 0.00014 mmol, 1.0 equiv), 129 μL of a 20 mg/mL solution of **AquaMet** in Milli-Q water (2.87 mg, 0.0036 mmol, 5.0 equiv relative to ~5 norbornene modifications per protein) was added to form **Lyz-MI** (Reaction scheme S1). It is assumed that all norbornenes are modified with the ruthenium catalyst. The reaction mixture was allowed to proceed at room temperature for 10 min. Reaction mixture was centrifuged at 10,000 × *g* for 5 min to remove any precipitates. The supernatant was distributed into 5× Amicon Ultra-0.5 mL Centrifugal Filters (200 μL each). 300 μL of 10 mM potassium phosphate buffer (pH 6.5) with 100 mM NaCl was also added into each of the filters, which were then centrifuged at 10,000 × *g* for 8 min. The concentrated **Lyz-MI** was washed three additional times in this manner, eluting with 10 mM potassium phosphate buffer (pH 6.5) with 100 mM NaCl, to remove excess catalyst while maintaining optimal catalyst activity. To each filter was added **NB-PEG** (500 mg/mL) as a solution in 10 mM potassium phosphate buffer (pH 6.5) with 100 mM NaCl: 0 equiv (2.4 μL, 1.12 mg, 0.0024 mmol, ~20 equiv relative to Ru per protein; 3.5 μL, 1.8 mg, 0.0036 mmol, ~30 equiv relative to Ru per protein; 5.9 μL, 3.0 mg, 0.0060 mmol, ~50 equiv relative to Ru per protein; 11.8 μL, 5.9 mg, 0.012 mmol, ~100 equiv relative to Ru per protein). Polymerizations were terminated after 1 h with the addition of 1 μL of diethylene glycol monovinyl ether. The resulting protein-polymer conjugates, **Lyz-PPC1**, were purified to remove any unreacted monomer by centrifugation and eluting with PBS (pH 7.4) three times. Resulting PPCs were analyzed by SDS-PAGE and SEC.

Polymerization procedure for synthesis of protein-block copolymer conjugates—To a 0.33 mL solution of **Lyz-NB** at a concentration of 2.0 mg/mL in 10 mM potassium phosphate buffer (pH 6.5) in 100 mM NaCl (0.71 mg, 0.00005 mmol, 1.0 equiv), 43 μL of a 20 mg/mL solution of **AquaMet** in Milli-Q water (0.86 mg, 0.001 mmol, 5.0 equiv relative to ~5 norbornene modifications per protein) was added to form **Lyz-MI** (Figure 1A). It is assumed that all norbornenes are modified with the ruthenium catalyst. The reaction mixture was allowed to proceed at room temperature for 10 min.

Reaction mixture was centrifuged at 10,000 × *g* for 5 min to remove any precipitates. The supernatant was transferred into Amicon Ultra-0.5 mL Centrifugal Filters. Two hundred and fifty microliters of 10 mM potassium phosphate buffer (pH 6.5) with 100 mM NaCl were also added into each of the filters, which were then centrifuged at 10,000 × *g* for 8 min. The concentrated **Lyz-MI** was washed three additional times in this manner, eluting with 10 mM potassium phosphate buffer (pH 6.5) and 100 mM NaCl, to remove excess catalyst while maintaining optimal catalyst activity. **NB-Zwit** (500 mg/mL) as a solution in 10 mM potassium phosphate buffer (pH 6.5) with 100 mM NaCl was then added to the macroinitiator solution (3.0 μL, 1.5 mg, 0.0042 mmol). After 20 min, an aliquot (30 μL) was removed and terminated with 1 μL of diethylene glycol monovinyl ether. After 25 min, an additional aliquot (30 μL) was removed and terminated with 1 μL of diethylene glycol monovinyl ether. **NB-PEG** (500 mg/mL) as a solution in 10 mM potassium phosphate buffer (pH 6.5) and 100 mM NaCl (2.1 μL, 1.1 mg, 0.0021 mmol) was then added and allowed to react at room temperature for 20 min. Polymerizations were then terminated with the addition of 1 μL of diethylene glycol monovinyl ether. The resulting protein-polymer conjugates, **Lyz-PPC1**, were purified to remove any unreacted monomer by centrifugation and eluting with PBS (pH 7.4) three times. Resulting PPCs were analyzed by SDS-PAGE and SEC.

Lysozyme activity assay—The activities of **Lyz** and **Lyz-PPC**s were assayed using glycol chitosan substrate. First, 0.05% (w/v) glycol chitosan solution was prepared in 100 mM acetate buffer (pH 5.5). Next, 1.52 mM potassium ferricyanide solution was freshly prepared in0.5 M sodium carbonate. The substrate solution (100 μL) was added to 10 μL of **Lyz** or **Lyz-PPC**s solution (2 mg/mL) and incubated at 40°C for 30 min. After incubation, 200 μL of potassium ferricyanide solution was added and immediately boiled for 15 min and then cooled down. Two hundred microliters of each solution was transferred to a 96-well plate, and the absorbance was measured at 420 nm.

Synthesis of grafting-from Qβ-PPCs

Qβ expression—Bacteriophage Qβ VLPs were expressed as previously reported.[65] In brief, the gene encoding the VLP (NCBI: P03615) was cloned into pDUET-1 expression vectors (GenScript Biotech) and expressed in BL21 (DE3) *E. coli* (New England BioLabs). Colonies were grown in LB medium (Thermo Fisher Scientific) with 50 μg mL^{-1} of kanamycin as the selection marker. Stocks were prepared and stored at −80°C in 20% (v/v) glycerol. On the day of use, the stocks were thawed and grown in 10 mL of MagicMedia (Invitrogen) with 50 μg mL^{-1} kanamycin for 16 h at 37°C and 250 rpm. The entire culture was then transferred to 200 mL of MagicMedia with 50 μg mL^{-1} kanamycin and incubated for 20–24 h at 37°C and 300 rpm. The cells were harvested from the medium through centrifugation at 5,000 × *g* for 20 min at 4°C, and the pellet was stored at −80°C overnight. The pellet was then resuspended in a solution of 10 mL of lysis buffer (Thermo Fisher Scientific) per gram of the cell pellet. Lysozyme (1 mg mL^{-1}) (GoldBio), DNase (2 μg mL^{-1}) (Promega), and $MgCl_2$ (2 mM) (Fisher Scientific) were added to the lysis buffer, and the entire solution was stirred at 37°C for 1 h at 100 rpm. The solution was then sonicated at Amp 30% with 5-s cycles for 10 min on ice to complete the lysis. The lysate was centrifuged at 5,000 × *g* for 20 min at 4°C and the supernatant was collected. The

VLPs were precipitated from the supernatant through the addition of 10% (w/v) PEG-8000 (Thermo Fisher Scientific) and incubated at 4°C for 12 h on a rotisserie. Following the incubation, the solution was centrifuged at 5,000 × *g* for 20 min at 4°C, and the pellet was dissolved in 5 mL of PBS, pH 7.4 (G Biosciences). A total of 2.5 mL of a 1:1 (v/v) mixture of butanol (Fisher Scientific) and chloroform (Fisher Scientific) was added to the PBS and centrifuged at 5,000 × *g* for 30 min at 4°C to remove any excess lipid. The supernatant was collected and purified through ultracentrifugation using a 10%–40% (w/v) sucrose (Sigma-Aldrich) gradient at 96,281 × *g* for 2.5 h at 4°C. The middle band, which is due to the light scattering by the Qβ VLPs, was collected and ultracentrifuged at 160,326 × *g* for 2.5 h at 4°C. The pelleted VLPs were resuspended in PBS (pH 7.4) and quantified using a Pierce BCA Protein Assay Kit (Thermo Fisher Scientific). VLPs to be used immediately were stored at 4°C; otherwise they were kept at −80°C until further use. Qβ was characterized by mass spectrometry (Figure S8), SEC (Figure S9), DLS (Figure S14A), and TEM (Figure S15A).

Synthesis of Qβ-NB—Qβ (20 mg, 0.0000078 mmol, 1 equiv) was dissolved in 10 mL of 0.1 M KPB (pH 8.0) buffer in a 20-mL glass scintillation vial and stirred for 5 min. To this solution, exo-NBDA (27.64 mg, 0.169 mmol, 21,600 equiv or 30 equiv/NH_2 residues) dissolved in 1.1 mL of anhydrous DMSO was added over a span of 60 min. After the overnight reaction, the product was dialyzed against 0.01 M KPB (pH 6.5), 0.1 M NaCl buffer in a 10 kDa MWCO dialysis tube to remove unreacted exo-NBDA and switch sample buffers. The dialyzed sample was concentrated in AMICON 4 mL 10 kDa MWCO centrifuge filters to a final volume of 1 mL. Protein concentration was analyzed using Bradford assay or BCA assay with BSA standards. Qβ-NB was characterized using SEC (Figure S11), SDS-PAGE (Figure 5B), mass spectrometry (Figure S10), DLS (Figure S14B), and TEM (Figure S15B).

Polymerization procedure for the synthesis of Qβ-PPC1 and Qβ-PPC2—Qβ-NB (15 mg, 0.0011 mmol, 1 equiv) was dissolved in 7.5 mL of 10 mM potassium phosphate buffer (pH 6.5), 100 mM M NaCl buffer (Reaction scheme S3). AquaMet (12.64 mg, 0.016 mmol, 5 equiv) was freshly dissolved in 632 μL of deionized water and added to the Qβ-NB solution and vortexed to mix. The reaction was carried out for 10 min. Tween 20 (0.1%, v/v) was added to the reaction mixture and vortexed. The mixture was then centrifuged at 10,000 × *g* for 5 min to remove any unreacted catalyst from the Qβ macroinitiator. The supernatant was then split into four equal volumes and washed in Amicon Ultra-0.5 mL 100 kDa MWCO centrifuge filters using the reaction buffer. Monomer NB-PEG (12.2 mg or 30 equiv and 40.52 mg or 100 equiv) was dissolved in 24.4 μL and 81.1 μL of anhydrous DMSO, respectively. Monomer NB-Zwit (8.5 mg or 30 equiv and 28.04 mg or 100 equiv) was dissolved in 17 μL and 56 μL of 10 mM potassium phosphate + 100 mM NaCl buffer (pH 6.5), respectively. The monomers were then added to the centrifuge filters with the macroinitiator and reacted for 40 min. Unreacted monomers were removed by washing with the reaction buffer repeated thrice. The conjugates were characterized using SDS-PAGE (Figure 5B), SEC (Figure 5C), DLS (Figures S14D–S14G), and TEM (Figures 5D–5G).

ELISA immune assay—Qβ was coated onto each well of the Thermo Scientific NUNC 96-well plates using coating buffer (0.1 M kP buffer, pH 7.0) overnight in a shaker at 4°C (10 μg Qβ/mL). The solution was removed by plate washer (accuWash from Fisher Scientific) and the wells were washed three times with 200 μL of wash solution (0.05% [w/v] Tween 20 in 1× PBS). The wells were coated with 100 μL of 3% BSA (w/v) in 1× PBS and left to shake overnight at 4°C. The washing protocol was repeated. Primary antibody solutions were prepared at 2.1 μg/mL with 5% BSA (w/v) in 1× PBS (for Qβ detection, rabbit-derived anti-Qβ antibody from Pacific Immunology Lot 13503/13504; for PEG detection, anti-PEG antibody clone 26A04 from BioVision). The solutions were added at a volume of 100 μL to the sample wells and left to incubate at 25°C under agitation for 1 h. The washing protocol was repeated. Secondary antibody solutions were prepared at 0.2 μg/mL with 5% BSA (w/v) in 1× PBS (for Qβ detection, goat anti-rabbit IgG [H + L] horseradish peroxidase [HRP] conjugates from Invitrogen, #65–6120; for PEG detection, goat anti-rat IgG [H + L] HRP from BioVision, #6908). The solutions were added at a volume of 100 μL to the sample wells and left to incubate at 25°C under agitation for 1 h. The washing protocol was repeated. Room temperature 1-Step Ultra TMB-ELISA Substrate Solution (Thermo Scientific, #34028) was added to the wells at 100 μL and left to react for 2 min. The reaction was quenched with 100 μL of 2 N H_2SO_4. The absorbance of the solutions at 650 nm was measured using a plate reader (Tecan Infinite M Plex).

Supplementary Material

Refer to Web version on PubMed Central for supplementary material.

ACKNOWLEDGMENTS

This work was sponsored primarily by the UC San Diego Materials Research Science and Engineering Center (UCSD MRSEC), supported by the National Science Foundation (DMR 2011924), as well as a grant by the NSF chemistry program (CHE 1808031). The authors would like to thank Dr. Ivonne Gonzalez Gamboa for assisting with the TEM protocol. The authors would like to thank the personnel (Ying Jones, Vanessa Taupin, and Guillaume Castillon) of the University of California, San Diego Cellular and Molecular Medicine Electron Microscopy Core Facility for technical assistance. The Cellular and Molecular Medicine EM core facility is supported in part by National Institutes of Health award number S10OD023527.

REFERENCES

1. Walsh G (2018). Biopharmaceutical benchmarks 2018. Nat. Biotechnol 36, 1136–1145. 10.1038/nbt.4305. [PubMed: 30520869]
2. Krejsa C, Rogge M, and Sadee W (2006). Protein therapeutics: new applications for pharmacogenetics. Nat. Rev. Drug Discov 5, 507–521. 10.1038/nrd2039. [PubMed: 16763661]
3. Leader B, Baca QJ, and Golan DE (2008). Protein therapeutics: a summary and pharmacological classification. Nat. Rev. Drug Discov 7, 21–39. 10.1038/nrd2399. [PubMed: 18097458]
4. Weng Z, and DeLisi C (2002). Protein therapeutics: promises and challenges for the 21st century. Trends Biotechnol. 20, 29–35. 10.1016/S0167-7799(01)01846-7. [PubMed: 11742675]
5. Grigoletto A, Maso K, Mero A, Rosato A, Schiavon O, and Pasut G (2016). Drug and protein delivery by polymer conjugation. J. Drug Deliv. Sci. Technol 32, 132–141. 10.1016/j.jddst.2015.08.006.
6. Kaupbayeva B, and Russell AJ (2020). Polymer-enhanced biomacromolecules. Prog. Polym. Sci 101, 101194. 10.1016/j.progpolymsci.2019.101194.

7. Ko JH, and Maynard HD (2018). A guide to maximizing the therapeutic potential of protein–polymer conjugates by rational design. Chem. Soc. Rev 47, 8998–9014. 10.1039/C8CS00606G. [PubMed: 30443654]
8. Abuchowski A, van Es T, Palczuk NC, and Davis FF (1977). Alteration of immunological properties of bovine serum albumin by covalent attachment of polyethylene glycol. J. Biol. Chem 252, 3578–3581. 10.1016/S0021-9258(17)40291-2. [PubMed: 405385]
9. Abuchowski A, McCoy JR, Palczuk NC, van Es T, and Davis FF (1977). Effect of covalent attachment of polyethylene glycol on immunogenicity and circulating life of bovine liver catalase. J. Biol. Chem 252, 3582–3586. 10.1016/S0021-9258(17)40292-4. [PubMed: 16907]
10. Lee PW, Isarov SA, Wallat JD, Molugu SK, Shukla S, Sun JEP, Zhang J, Zheng Y, Lucius Dougherty M, Konkolewicz D, et al. (2017). Polymer structure and conformation alter the antigenicity of virus-like particle–polymer conjugates. J. Am. Chem. Soc 139, 3312–3315. 10.1021/jacs.6b11643. [PubMed: 28121424]
11. Crooke SN, Zheng J, Ganewatta MS, Guldberg SM, Reineke TM, and Finn MG (2019). Immunological properties of protein–polymer nanoparticles. ACS Appl. Bio Mater 2, 93–103. 10.1021/acsabm.8b00418.
12. Harris JM, and Chess RB (2003). Effect of pegylation on pharmaceuticals. Nat. Rev. Discov 2, 214–221. 10.1038/nrd1033.
13. Pelegri-O'Day EM, Lin E-W, and H. D (2014). Therapeutic protein–polymer conjugates: advancing beyond PEGylation. J. Am. Chem. Soc 136, 14323–14332. 10.1021/ja504390x. [PubMed: 25216406]
14. Veronese FM, and Mero A (2008). The impact of PEGylation on biological therapies. BioDrugs 22, 315–329. 10.2165/00063030-200822050-00004. [PubMed: 18778113]
15. Moncalvo F, Martinez Espinoza MI, and Cellesi F (2020). Nanosized delivery systems for therapeutic proteins: clinically validated Technologies and advanced development strategies. Front. Bioeng. Biotechnol 8, 89. [PubMed: 32117952]
16. Lipsky PE, Calabrese LH, Kavanaugh A, Sundy JS, Wright D, Wolfson M, and Becker MA (2014). Pegloticase immunogenicity: the relationship between efficacy and antibody development in patients treated for refractory chronic gout. Arthritis Res. Ther 16, R60. 10.1186/ar4497. [PubMed: 24588936]
17. Schlesinger N, and Lipsky PE (2020). Pegloticase treatment of chronic refractory gout: update on efficacy and safety. Semin. Arthritis Rheum 50, S31–S38. 10.1016/j.semarthrit.2020.04.011. [PubMed: 32620200]
18. Armstrong JK, Hempel G, Koling S, Chan LS, Fisher T, Meiselman HJ, and Garratty G (2007). Antibody against poly(ethylene glycol) adversely affects PEG-asparaginase therapy in acute lymphoblastic leukemia patients. Cancer 110, 103–111. 10.1002/cncr.22739. [PubMed: 17516438]
19. Richter AW, and Åkerblom E (1984). Polyethylene glycol reactive antibodies in man: titer distribution in allergic patients treated with monomethoxy polyethylene glycol modified allergens or placebo, and in healthy blood donors. Int. Arch. Allergy Appl. Immunol 74, 36–39. 10.1159/000233512. [PubMed: 6706424]
20. Garay RP, El-Gewely R, Armstrong JK, Garratty G, and Richette P (2012). Antibodies against polyethylene glycol in healthy subjects and in patients treated with PEG-conjugated agents. Expert Opin. Drug Deliv 9, 1319–1323. 10.1517/17425247.2012.720969. [PubMed: 22931049]
21. Chen B-M, Su Y-C, Chang C-J, Burnouf P-A, Chuang K-H, Chen C-H, Cheng T-L, Chen Y-T, Wu J-Y, and Roffler SR (2016). Measurement of pre-existing IgG and IgM antibodies against polyethylene glycol in healthy individuals. Anal. Chem 88, 10661–10666. 10.1021/acs.analchem.6b03109. [PubMed: 27726379]
22. Yang Q, Jacobs TM, McCallen JD, Moore DT, Huckaby JT, Edelstein JN, and Lai SK (2016). Analysis of pre-existing IgG and IgM antibodies against polyethylene glycol (PEG) in the general population. Anal. Chem 88, 11804–11812. 10.1021/acs.analchem.6b03437. [PubMed: 27804292]
23. Yang Q, and Lai SK (2015). Anti-PEG immunity: emergence, characteristics, and unaddressed questions. Wiley Interdiscip. Rev. Nanomed. Nanobiotechnol 7, 655–677. 10.1002/wnan.1339. [PubMed: 25707913]

24. Kozma GT, Shimizu T, Ishida T, and Szebeni J (2020). Anti-PEG antibodies: properties, formation, testing and role in adverse immune reactions to PEGylated nanobiopharmaceuticals. Adv. Drug Deliv. Rev 154–155, 163–175. 10.1016/j.addr.2020.07.024.
25. Dams ET, Laverman P, Oyen WJ, Storm G, Scherphof GL, van Der Meer JW, Corstens FH, and Boerman OC (2000). Accelerated blood clearance and altered biodistribution of repeated injections of sterically stabilized liposomes. J. Pharmacol. Exp. Ther 292, 1071–1079. [PubMed: 10688625]
26. McSweeney MD, Mohan M, Commins SP, and Lai SK (2021). Anaphylaxis to Pfizer/BioNTech mRNA COVID-19 vaccine in a patient with clinically confirmed PEG allergy. Front. Allergy 2, 715844. [PubMed: 35387046]
27. Sellaturay P, Nasser S, Islam S, Gurugama P, and Ewan PW (2021). Polyethylene glycol (PEG) is a cause of anaphylaxis to the Pfizer/BioNTech mRNA COVID-19 vaccine. Clin. Exp. Allergy 51, 861–863. 10.1111/cea.13874. [PubMed: 33825239]
28. Zalipsky S (1995). Chemistry of polyethylene glycol conjugates with biologically active molecules. Adv. Drug Deliv. Rev 16, 157–182. 10.1016/0169-409X(95)00023-Z.
29. Obermeyer AC, and Olsen BD (2015). Synthesis and application of protein-containing block copolymers. ACS Macro Lett. 4, 101–110. 10.1021/mz500732e. [PubMed: 35596389]
30. Falatach R, McGlone C, Al-Abdul-Wahid MS, Averick S, Page RC, Berberich JA, and Konkolewicz D (2015). The best of both worlds: active enzymes by grafting-to followed by grafting-from a protein. Chem. Commun 51, 5343–5346. 10.1039/C4CC09287B.
31. Cobo I, Li M, Sumerlin BS, and Perrier S (2015). Smart hybrid materials by conjugation of responsive polymers to biomacromolecules. Nat. Mater 14, 143–159. 10.1038/nmat4106. [PubMed: 25401924]
32. Paeth M, Stapleton J, Dougherty ML, Fischesser H, Shepherd J, McCauley M, Falatach R, Page RC, Berberich JA, and Konkolewicz D (2017). Chapter nine - approaches for conjugating tailor-made polymers to proteins. In Methods in Enzymology NanoArmoring of Enzymes: Rational Design of Polymer-Wrapped Enzymes, Kumar CV, ed. (Academic Press), pp. 193–224. 10.1016/bs.mie.2016.12.004.
33. Wright TA, Page RC, and Konkolewicz D (2019). Polymer conjugation of proteins as a synthetic post-translational modification to impact their stability and activity. Polym. Chem 10, 434–454. 10.1039/C8PY01399C. [PubMed: 31249635]
34. Wang Y, and Wu C (2018). Site-specific conjugation of polymers to proteins. Biomacromolecules 19, 1804–1825. 10.1021/acs.biomac.8b00248. [PubMed: 29722971]
35. Wallat JD, Rose KA, and Pokorski JK (2014). Proteins as substrates for controlled radical polymerization. Polym. Chem 5, 1545–1558. 10.1039/C3PY01193C.
36. Messina MS, Messina KMM, Bhattacharya A, Montgomery HR, and Maynard HD (2020). Preparation of biomolecule-polymer conjugates by grafting-from using ATRP, RAFT, or ROMP. Prog. Polym. Sci 100, 101186. 10.1016/j.progpolymsci.2019.101186. [PubMed: 32863465]
37. Li H, Li M, Yu X, Bapat AP, and Sumerlin BS (2011). Block copolymer conjugates prepared by sequentially grafting from proteinsvia RAFT. Polym. Chem 2, 1531–1535. 10.1039/C1PY00031D.
38. Tucker BS, Coughlin ML, Figg CA, and Sumerlin BS (2017). Grafting-from proteins using metal-free PET–RAFT polymerizations under mild visible-light irradiation. ACS Macro Lett. 6, 452–457. 10.1021/acsmacrolett.7b00140. [PubMed: 35610863]
39. Kovaliov M, Allegrezza ML, Richter B, Konkolewicz D, and Averick S (2018). Synthesis of lipase polymer hybrids with retained or enhanced activity using the grafting-from strategy. Polymer 137, 338–345. 10.1016/j.polymer.2018.01.026.
40. Baker SL, Kaupbayeva B, Lathwal S, Das SR, Russell AJ, and Matyjaszewski K (2019). Atom transfer radical polymerization for biorelated hybrid materials. Biomacromolecules 20, 4272–4298. 10.1021/acs.biomac.9b01271. [PubMed: 31738532]
41. Olson RA, Korpusik AB, and Sumerlin BS (2020). Enlightening advances in polymer bioconjugate chemistry: light-based techniques for grafting to and from biomacromolecules. Chem. Sci 11, 5142–5156. 10.1039/D0SC01544J. [PubMed: 34122971]

42. Isarov SA, and Pokorski JK (2015). Protein ROMP: aqueous graft-from ring-opening metathesis polymerization. ACS Macro Lett. 4, 969–973. 10.1021/acsmacrolett.5b00497. [PubMed: 35596466]
43. Isarov SA, Lee PW, and Pokorski JK (2016). Graft-to" protein/polymer conjugates using polynorbornene block copolymers. Biomacromolecules 17, 641–648. 10.1021/acs.biomac.5b01582. [PubMed: 26765848]
44. Church DC, and Pokorski JK (2020). Cell engineering with functional poly(oxanorbornene) block copolymers. Angew. Chem. Int. Ed. Engl 59, 11379–11383. 10.1002/anie.202005148. [PubMed: 32281276]
45. Gallivan JP, Jordan JP, and Grubbs RH (2005). A neutral, water-soluble olefin metathesis catalyst based on an N-heterocyclic carbene ligand. Tetrahedron Lett. 46, 2577–2580. 10.1016/j.tetlet.2005.02.096.
46. Mayer C, Gillingham DG, Ward TR, and Hilvert D (2011). An artificial metalloenzyme for olefin metathesis. Chem. Commun 47, 12068–12070. 10.1039/C1CC15005G.
47. Sauer DF, Himiyama T, Tachikawa K, Fukumoto K, Onoda A, Mizohata E, Inoue T, Bocola M, Schwaneberg U, Hayashi T, and Okuda J (2015). A highly active biohybrid catalyst for olefin metathesis in water: impact of a hydrophobic cavity in a β-barrel protein. ACS Catal. 5, 7519–7522. 10.1021/acscatal.5b01792.
48. Sauer DF, Gotzen S, and Okuda J (2016). Metatheases: artificial metalloproteins for olefin metathesis. Org. Biomol. Chem 14, 9174–9183. 10.1039/C6OB01475E. [PubMed: 27545851]
49. Masuda S, Tsuda S, and Yoshiya T (2018). Ring-closing metathesis of unprotected peptides in water. Org. Biomol. Chem 16, 9364–9367. 10.1039/C8OB02778A. [PubMed: 30516782]
50. Trnka TM, and Grubbs RH (2001). The development of L2X2RuCHR olefin metathesis catalysts: an organometallic success story. Acc. Chem. Res 34, 18–29. 10.1021/ar000114f. [PubMed: 11170353]
51. Samanta D, Kratz K, Zhang X, and Emrick T (2008). A synthesis of PEG- and phosphorylcholine-substituted pyridines to afford water-soluble ruthenium benzylidene metathesis catalysts. Macromolecules 41, 530–532. 10.1021/ma7019732.
52. Breitenkamp K, and Emrick T (2005). Amphiphilic ruthenium benzylidene metathesis catalyst with PEG-substituted pyridine ligands. J. Polym. Sci. A Polym. Chem 43, 5715–5721. 10.1002/pola.21061.
53. Church DC, Takiguchi L, and Pokorski JK (2020). Optimization of ring-opening metathesis polymerization (ROMP) under physiologically relevant conditions. Polym. Chem 11, 4492–4499. 10.1039/D0PY00716A. [PubMed: 33796158]
54. Foster JC, Grocott MC, Arkinstall LA, Varlas S, Redding MJ, Grayson SM, and O'Reilly RK (2020). It is better with salt: aqueous ring-opening metathesis polymerization at neutral pH. J. Am. Chem. Soc 142, 13878–13885. 10.1021/jacs.0c05499. [PubMed: 32673484]
55. Steinmetz NF (2010). Viral nanoparticles as platforms for next-generation therapeutics and imaging devices. Nanomedicine 6, 634–641. 10.1016/j.nano.2010.04.005. [PubMed: 20433947]
56. Pokorski JK, and Steinmetz NF (2011). The art of engineering viral nanoparticles. Mol. Pharm 8, 29–43. 10.1021/mp100225y. [PubMed: 21047140]
57. Kurfürst MM (1992). Detection and molecular weight determination of polyethylene glycolmodified hirudin by staining after sodium dodecyl sulfate-polyacrylamide gel electrophoresis. Anal. Biochem 200, 244–248. 10.1016/0003-2697(92)90460-O. [PubMed: 1378701]
58. González-Gamboa I, Manrique P, Sánchez F, and Ponz F (2017). Plant-made potyvirus-like particles used for log-increasing antibody sensing capacity. J. Biotechnol 254, 17–24. 10.1016/j.jbiotec.2017.06.014. [PubMed: 28625680]
59. Tkachenko V, Vidal L, Josien L, Schmutz M, Poly J, and Chemtob A (2020). Characterizing the core-shell architecture of block copolymer nanoparticles with electron microscopy: a multi-technique approach. Polymers 12, 1656. 10.3390/polym12081656. [PubMed: 32722462]
60. Georgiev GS, Kamenska EB, Vassileva ED, Kamenova IP, Georgieva VT, Iliev SB, and Ivanov IA (2006). Self-assembly, antipolyelectrolyte effect, and nonbiofouling properties of polyzwitterions. Biomacromolecules 7, 1329–1334. 10.1021/bm050938q. [PubMed: 16602757]

61. Keefe AJ, and Jiang S (2011). Poly(zwitterionic)protein conjugates offer increased stability without sacrificing binding affinity or bioactivity. Nat. Chem 4, 59–63. 10.1038/nchem.1213. [PubMed: 22169873]

62. Qi Y, Simakova A, Ganson NJ, Li X, Luginbuhl KM, Özer I, Liu W, Hershfield MS, Matyjaszewski K, and Chilkoti A (2016). A brush-polymer/exendin-4 conjugate reduces blood glucose levels for up to five days and eliminates poly(ethylene glycol) antigenicity. Nat. Biomed. Eng 1, 0002–0012. 10.1038/s41551-016-0002. [PubMed: 28989813]

63. Han Y, Yuan Z, Zhang P, and Jiang S (2018). Zwitterlation mitigates protein bioactivity loss in vitro over PEGylation. Chem. Sci 9, 8561–8566. 10.1039/C8SC01777H. [PubMed: 30568780]

64. Birchall LT, Shehata S, Serpell CJ, Clark ER, and Biagini SCG (2021). Himic anhydride: a retro diels–alder reaction for the organic laboratory and an accompanying NMR study. J. Chem. Educ 98, 4013–4016. 10.1021/acs.jchemed.1c00661. [PubMed: 34924600]

65. Brown SD, Fiedler JD, and Finn MG (2009). Assembly of hybrid bacteriophage Qβ virus-like particles. Biochemistry 48, 11155–11157. 10.1021/bi901306p. [PubMed: 19848414]

Highlights

- Polynorbornene-based PPCs are synthesized using living aqueous grafting-from ROMP
- Synthesized PPCs retain nearly 100% bioactivity
- Synthesized PPCs evade recognition by protein-specific and PEG-specific antibodies
- Synthesized PPCs could be potential PEG alternatives in protein therapeutics

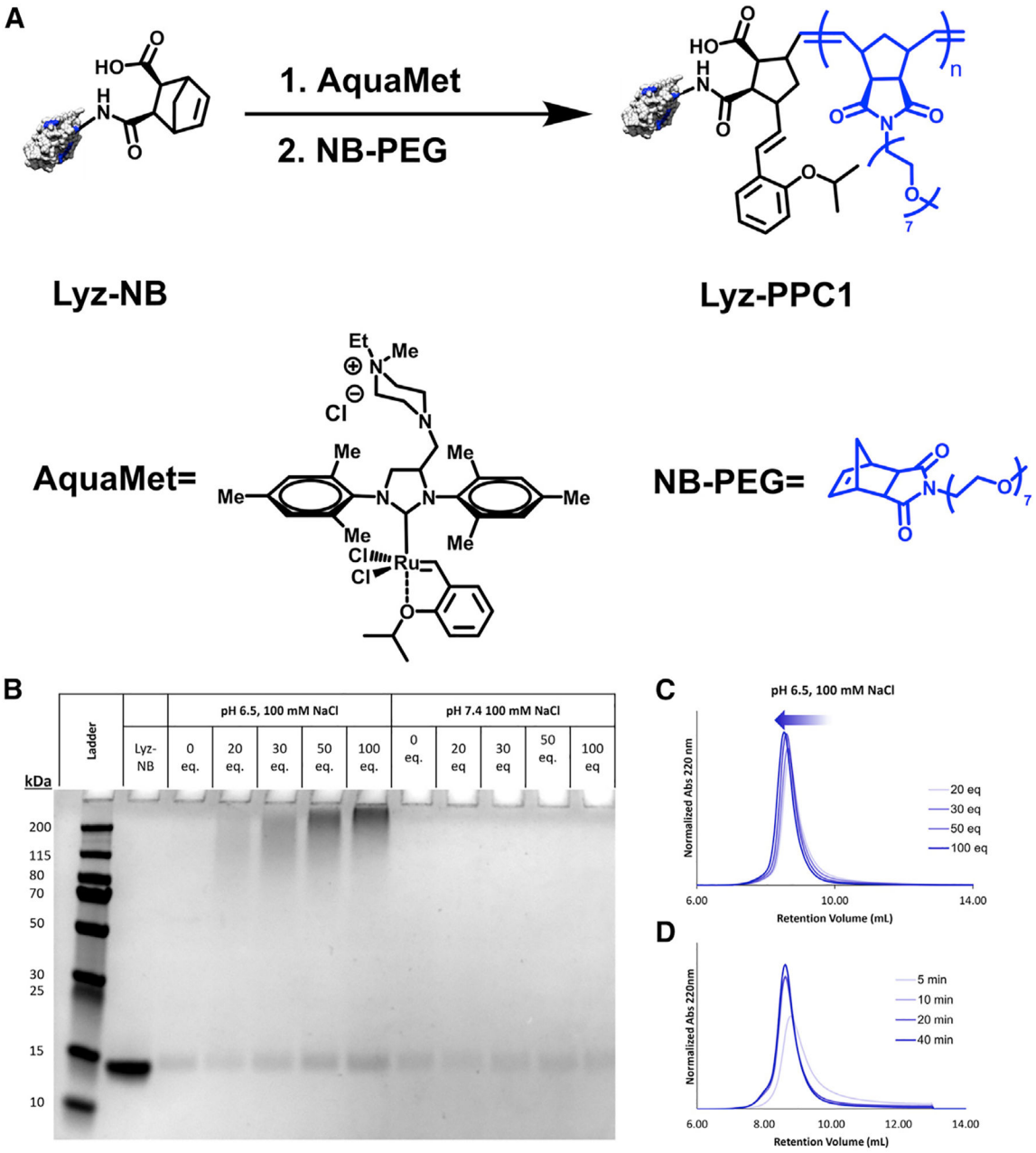

Figure 1. Synthesis and characterization of Lyz-PPC1

(A) Reaction scheme for synthesis of Lyz-PPC1.

(B) Denaturing SDS-PAGE gel comparing synthesis of Lyz-PPC1 in potassium phosphate buffer at pH 6.5 and pH 7.4 in 100 mM NaCl.

(C) SEC trace of Lyz-PPC1 synthesized with 20, 30, 50, and 100 equiv of NB-PEG. Absorbance detected at 220 nm. Lyz-NB trace also included for comparison.

(D) SEC trace of the polymerization of Lyz-PPC1 at different reaction time points. Absorbance detected at 220 nm.

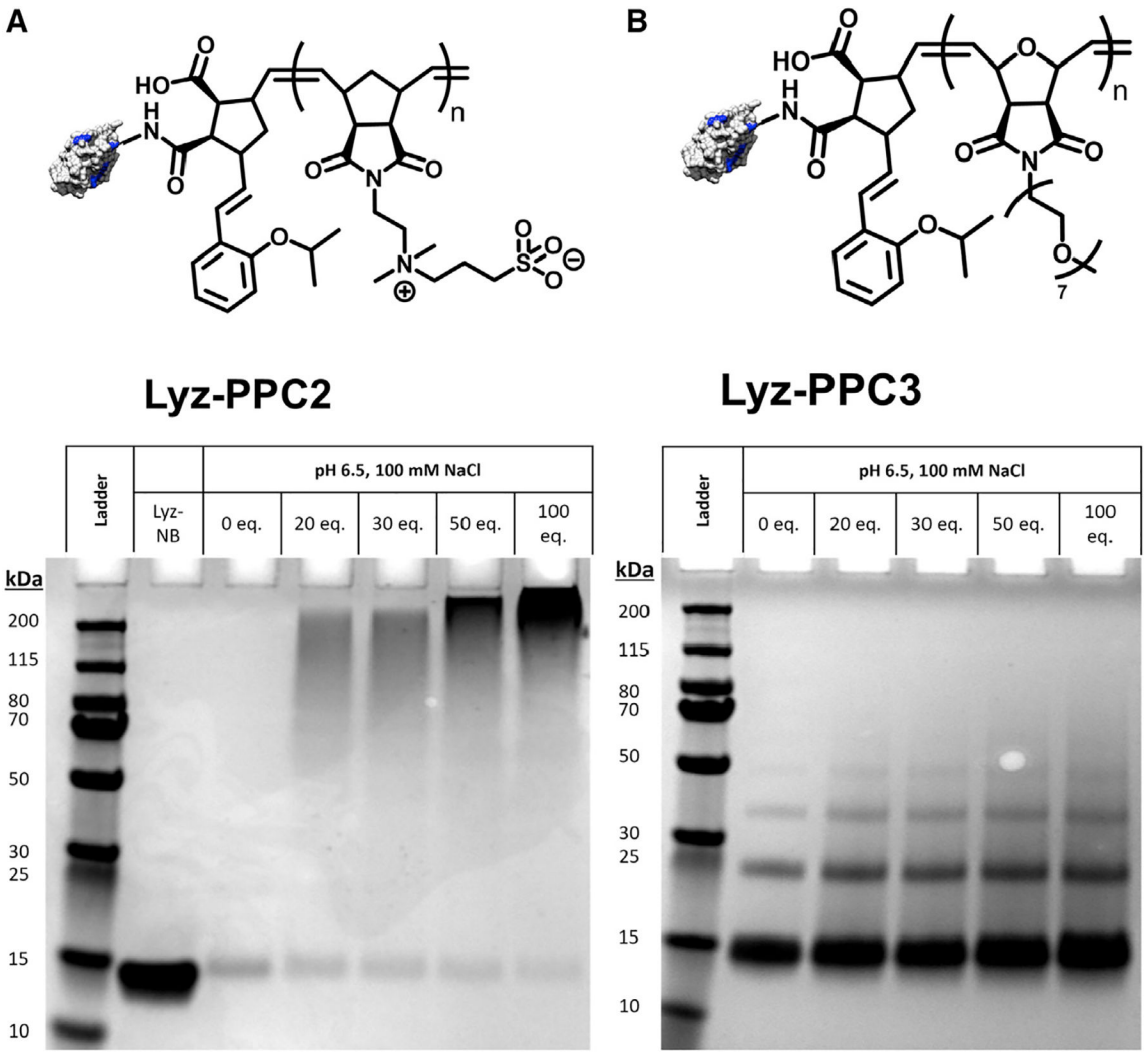

Figure 2. Characterization of Lyz-PPC2 and Lyz-PPC3 by denaturing SDS-PAGE gel

(A and B) SDS-PAGE of Lyz-PPC2 synthesized from NB-Zwit (A) and Lyz-PPC3 (B). Monomers were added at 0, 20, 30, 50, and 100 equivalences relative to NBs modified on the protein surface.

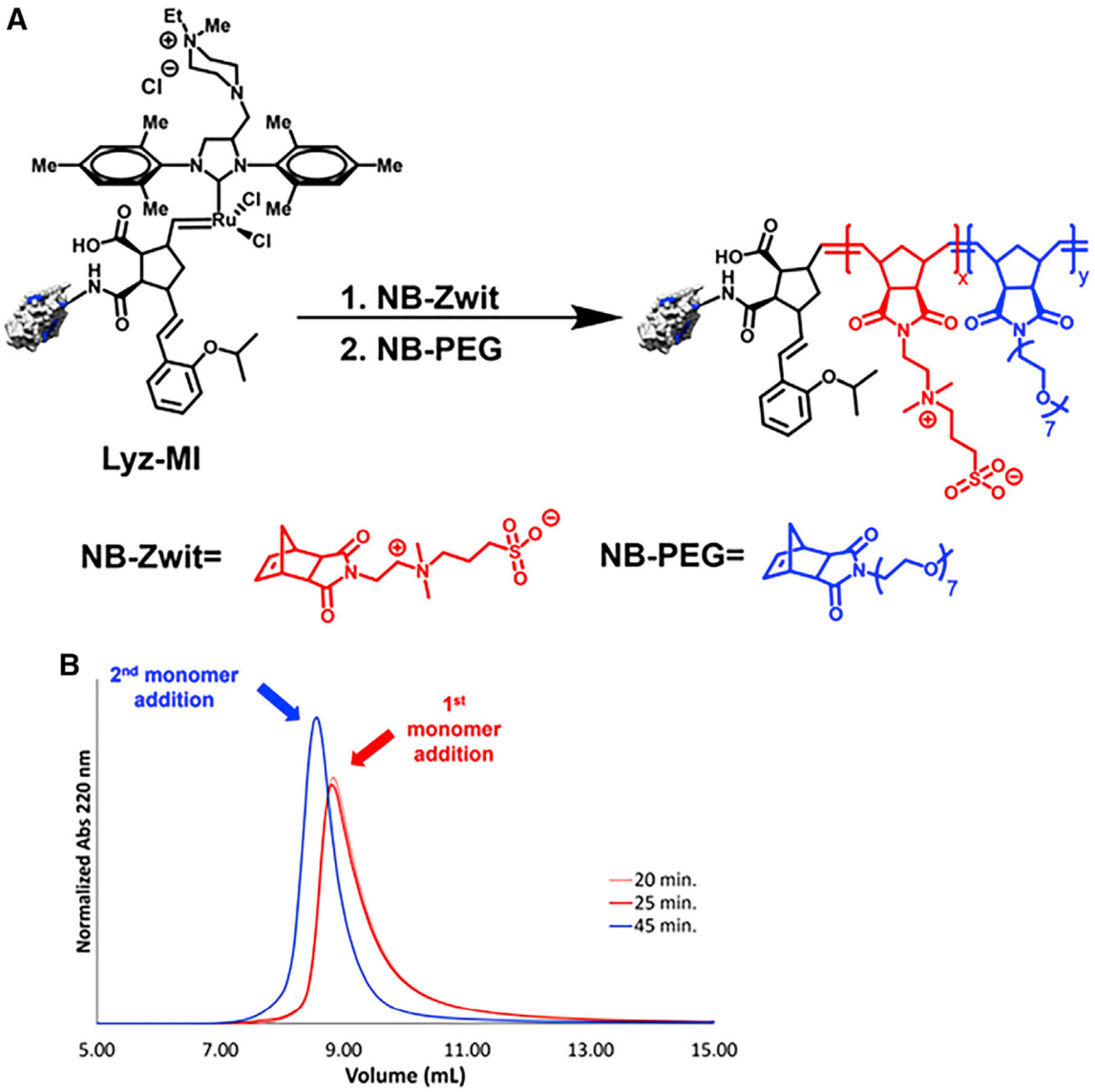

Figure 3. Synthesis and characterization of block copolymer protein conjugates

(A) Reaction scheme for synthesis of Lyz block copolymer conjugates.

(B) SEC trace of polymerization after first (NB-Zwit) and second (NB-PEG) monomer additions.

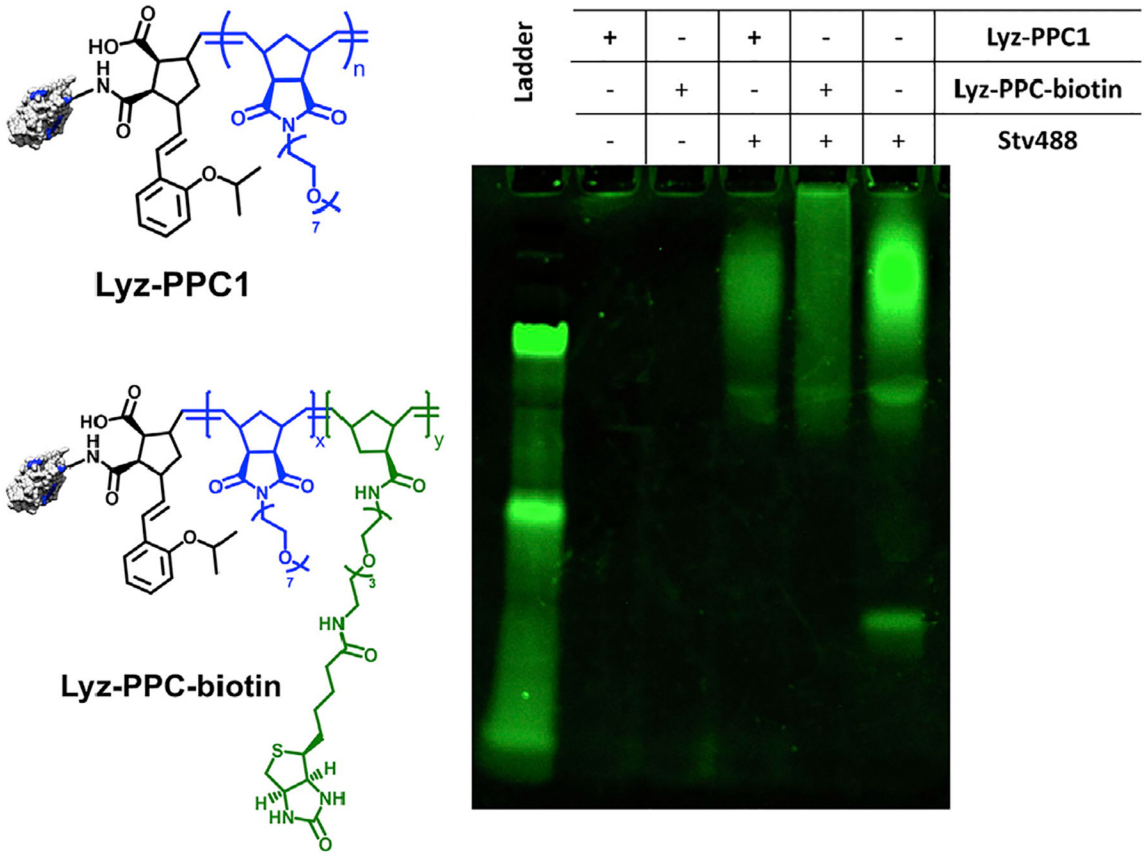

Figure 4. Characterization of Lyz-PPC-biotin by non-denaturing PAGE gel

The binding of Lyz-PPC-biotin to Stv488 was analyzed by the fluorescent imaging of the PAGE gel. The binding of Lyz-PPC1 to Stv488 was also analyzed for comparison.

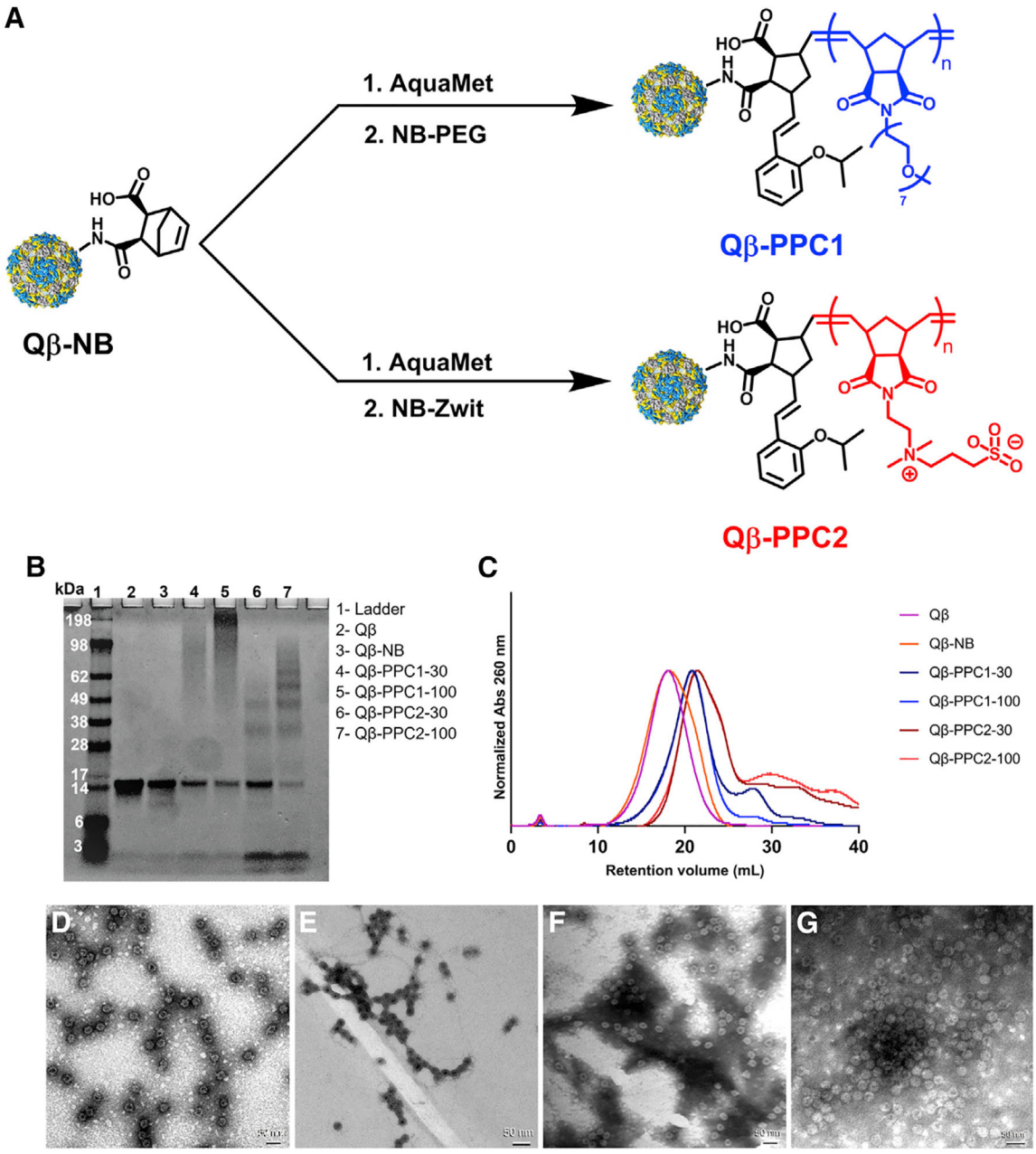

Figure 5. Synthesis and characterization of Qβ-PPCs

(A) Reaction scheme for the synthesis of Qβ-PPC1 and Qβ-PPC2.

(B) Denaturing SDS-PAGE of Qβ-PPC1 and Qβ-PPC2 in potassium phosphate buffer at pH 6.5, in 100 mM NaCl. Qβ-WT and Qβ-NB were also included for comparison. Samples were used at 0.05 mg/mL. The band at 14 kDa indicates Qβ coat protein.

(C) SEC trace of Qβ-PPC1 and Qβ-PPC2. Absorbance was detected at 260 nm. The Qβ-WT and Qβ-NB traces were also included for comparison.

(D–G) TEM micrographs of Qβ-PPC1–30 (D), Qβ-PPC1–100 (E), Qβ-PPC2–30 (F), and Qβ-PPC2–100 (G). TEM images were assessed at 49,000× magnification. Scale bars, 50 nm.

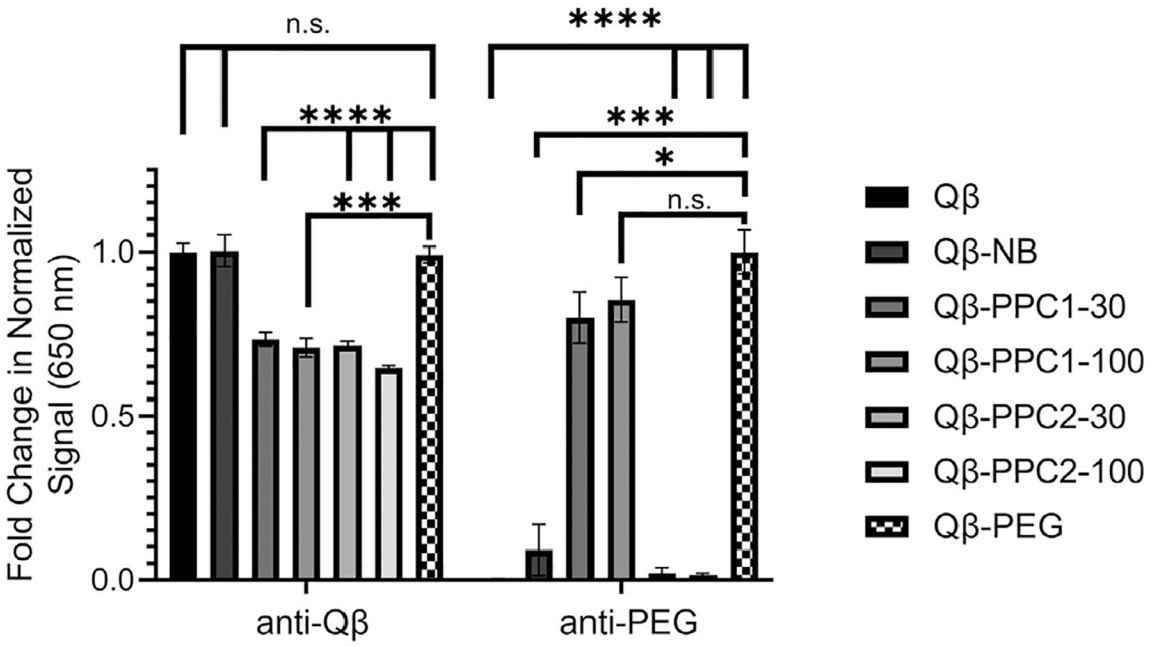

Figure 6. ELISA response of Qβ-PPCs toward anti-Qβ and anti-PEG

Results are normalized to immune response by Qβ-WT. The fold change in absorbance signal intensity as measured at 650 nm for each Qβ sample relative to the grafting-to Qβ-PEG positive control as determined by an anti-Qβ (left) and anti-PEG (right) indirect ELISAs. The significance measurements were determined by an unpaired t test relative to the positive control. The significance markers indicate no significant differences (n.s.), and *$p < 0.1$, **$p < 0.01$, ***$p < 0.001$, and ****$p < 0.0001$. Error bars denote SD; $N = 3$.